



International Conference  
Nuclear Energy for New Europe

## **A Mechanistic Bubble Force Model for the Development of Boiling Parameters in High Heat Flux Regimes**

**<sup>a,b</sup>Aljoša Gajšek**

<sup>a</sup>Faculty of Mathematics and Physics  
Jadranska ulica 19  
1000, Ljubljana, Slovenia  
aljosa.gajsek@ijs.si

**<sup>b</sup>Matej Tekavčič, <sup>a,b</sup>Boštjan Končar**

<sup>b</sup>Jožef Stefan Institute  
Jamova cesta 39  
1000, Ljubljana, Slovenia  
matej.tekavcic@ijs.si, bostjan.koncar@ijs.si

### **ABSTRACT**

In this work a mechanistic bubble force model has been studied aiming to identify the most important forces acting on a nucleating bubble. A python script has been developed to implement the model. The effects and significance of each force acting on a nucleating bubble under varied operating conditions have been evaluated. A particular emphasis was placed on the calculation of boiling parameters, i.e. bubble bubble liftoff detachment diameter, from these forces.

### **1 INTRODUCTION**

Nucleate boiling stands as a highly efficient heat transfer mechanism, capable to remove substantial quantities of energy from a heated surface while only prompting a minimal rise in surface temperature. However, a too high heat flux at the surface can lead to the occurrence of boiling crisis. This phenomenon transpires when the heated surface becomes crowded with emerging bubbles that coalesce into an insulating vapor layer. Subsequently, this is followed by a dramatic increase in the wall temperature, resulting in damage of the heated structures.

An insufficient understanding and prediction of the boiling process and the Critical Heat Flux (CHF) often results in costly and overly conservative solutions. Such designs are purposefully circumventing the boiling process altogether, operating in a single-phase convection mode only, instead of embracing the potential effectiveness of boiling heat transfer. This is also the case in the design of fusion divertors.

The heat flux received by the heated wall serves as an energy boundary condition within the Navier-Stokes equation. A mechanistic boiling model partitiones this heat flux into evaporation, single-phase convection, and quenching. The model then calculates the distribution of heat between liquid heating and vapor formation, a computation dependent on three key boiling parameters: nucleation site density, bubble detachment frequency, and bubble detachment diameter. Understanding and quantifying these parameters is therefore essential for accurate modeling of boiling flow.

In this work, a python script has been developed to implement the mechanistic bubble force model. We aim to quantify the effects and significance of specific forces acting on a nucleating bubble under varied operating conditions. A particular emphasis is placed on the calculation of bubble detachment diameter by sliding and liftoff from these forces. Ultimately, our research seeks to mitigate the existing disparity in the modeling of boiling flows in high heat flux and high flow velocity conditions.

## 2 MECHANISTIC BUBBLE FORCE MODEL

The mechanistic bubble force model was first introduced by Klausner [1] in 1993 and was later improved by Zeng *et al.* [2, 3]. More recently the model was adapted [4, 5, 6] to predict realistic boiling parameters for Eulerian multiphase computational fluid dynamics closure relations in various operating conditions. Different implementations of the model differ in their individual force models and computational methods used to calculate the bubble sliding diameter ( $d_{ds}$ ) or bubble liftoff diameter ( $d_{dl}$ ).

### 2.1 Bubble forces

A bubble growing on a heated surface in a convective flow is subjected to various forces, produced by interaction between the vapor, liquid and the solid. The most important forces are presented in Figure 1. The  $x$ -axis represents the stream-wise direction, and the  $y$ -axis represents the wall-normal direction.  $F_{gr}$  is growth force,  $F_{bouy}$  is buoyancy force,  $F_{drag}$  is drag force,  $F_{lift}$  is lift force and  $F_{st}$  is surface tension force. Forces that separate the bubble from the wall are presented in red, and forces that retain the bubble on the wall are in blue. The angles represent:  $\phi$  bubble inclination,  $\beta$  advancing angle, and  $\alpha$  rescinding angle.

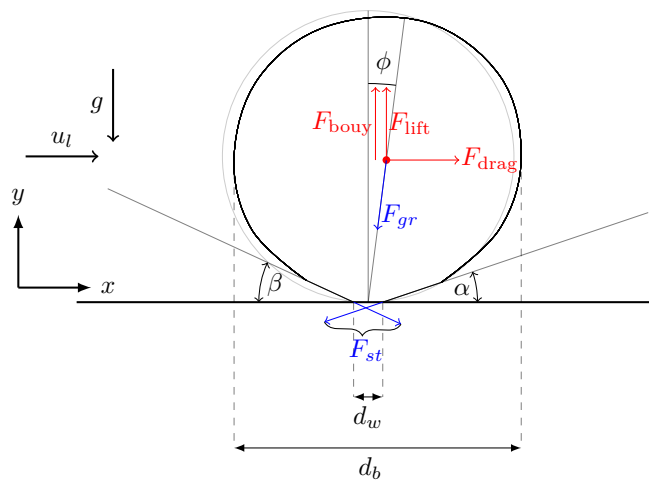


Figure 1: Forces acting on a growing bubble on the wall.

Growth force represents the resistance of the surrounding liquid, being pushed away by the growing bubble. Growth force of a hemispherical bubble acting on a stagnant fluid can be calculated as [6]

$$\vec{F}_{gr} = -\rho_l \pi d_w^2 \left[ r \dot{r} + \frac{3}{2} \dot{r}^2 \right] \vec{e}_y, \quad (1)$$

where  $\rho_l$  is liquid density,  $d_w$  is contact diameter between bubble and the surface,  $r$  is radius, and  $\vec{e}_y$  is a wall-normal unit vector. The key component of a bubble growth is a time dependent

radius estimation  $r(t)$ . In this work, an analytical solution for diffusion-controlled bubble growth in a super-heated liquid, derived by Cooper [7], was chosen as

$$r(t) = \frac{\eta_l}{0.804\sqrt{Pr}} Ja_{\text{sup}} \sqrt{t}, \quad (2)$$

where  $\eta_l$  is liquid thermal diffusivity,  $Pr$  is Prandtl number,  $Ja_{\text{sup}}$  super-heat Prandtl number and  $t$  time. Due to bubbles asymmetrical shape in a convective flow the growth force can get a stream-wise ( $F_{gr,x}$ ) and wall-normal ( $F_{gr,y}$ ) component based on inclination angle  $\phi$ .

Buoyancy force on a growing bubble can be expressed as

$$\vec{F}_{\text{bouy}} = \frac{4r^3}{3} (\rho_l - \rho_v) \vec{g}, \quad (3)$$

where  $\rho_v$  is vapour density and  $\vec{g}$  is gravitational acceleration.

Drag force on a growing bubble is calculated as

$$\vec{F}_{\text{drag}} = \frac{1}{2} C_D (\vec{v}_l - \vec{v}_b)^2, \quad (4)$$

where  $C_D$  is a drag coefficient and  $\vec{v}_l$  and  $\vec{v}_b$  are liquid and bubble velocities, respectively. The drag coefficient is calculated as [8]

$$C_D = 1.13 \frac{24}{Re_b} \left(1 + 0.104 Re_b^{0.753}\right), \quad (5)$$

Where  $Re_b = \frac{d|\vec{v}_l - \vec{v}_b| \rho_l}{\mu_l}$ , is bubble Reynolds number, and  $\mu_l$  is liquid's viscosity. The liquid velocity at the middle of the bubble has been used for calculation of drag force.

Velocity gradient due to the shear stress produces a lift force that is pulling the bubble away from the wall. The lift force is calculated similarly as the drag force, look Eq. (4), but substituting  $C_D$  for  $C_L$ , that is lift coefficient, and can be expressed as [9]

$$C_L = 3.877 G_s^{\frac{1}{2}} \left[ Re_b^{-2} + 0.014 G_s^2 \right]^{\frac{1}{4}}, \quad (6)$$

where  $G_s = \left| \frac{dU}{dy} \right| \frac{r}{|v_l - v_b|}$ . The calculation of  $\frac{dU}{dy}$  requires a velocity profile, which has been calculated using single phase wall functions for turbulent flow proposed by Situ [10]. The liquid velocity at the top of the bubble has been used for calculation of lift force in Eq. (4).

Klausner [1] has proposed the following models for surface tension forces in stream-wise and wall-normal directions

$$F_{st,x} = -d_w \sigma \frac{\pi(\alpha - \beta)}{\pi^2 - (\alpha - \beta)} [\sin \alpha + \sin \beta], \quad (7)$$

$$F_{st,y} = -d_w \sigma \frac{\pi}{\alpha - \beta} [\cos \beta - \cos \alpha], \quad (8)$$

where  $\sigma$  is surface tension.

## 2.2 Fluid properties

Both liquid and vapor properties have been determined using a CoolProp library [11] therefore all properties are temperature and pressure dependent. Liquid properties have been selected at  $T_l = T_{\text{sat}} - 10$  K and vapor is always assumed to be at saturation conditions therefore all properties have been selected at  $T_v = T_{\text{sat}}$ . The working fluid in this study is water.

## 2.3 Model constants

Some of the model parameters proved can be very challenging to adequately model, therefore they have been fixed to a constant value for the sake of simplicity of model analysis. As suggested by the work of Klausner [1], a constant values have been chosen for  $\alpha = \frac{\pi}{5}$ ,  $\beta = \frac{\pi}{4}$ ,  $d_w = 0.09$  mm and  $\phi = \frac{\pi}{18}$ .

It's crucial to acknowledge that while these constants simplify the model, they also influence the outcomes of the simulations. Since the individual forces in the model are heavily dependent on these constants, variations in their values could lead to significant changes in the model's predictions. Thus, while our model provides valuable insights, it should be applied in real-world contexts with a clear understanding of these inherent simplifications.

## 2.4 Calculation of bubble departure diameter

Schematics of bisection algorithm used to calculate bubble departure diameter are presented in Figure 2. Due to the critical role of bubble relative velocity in drag and lift force (see Eq. [4, 5, 6]), it needs to be calculated for each bubble size larger than  $d_{ds}$ . The bubble begins to slide when the sum of forces in stream-wise direction is larger than 0, that is

$$\sum F_y = F_{st,y} + F_{gr,y} + F_{drag} > 0. \quad (9)$$

For bubbles larger than the  $d_{ds}$ , the bubble velocity  $\vec{v}_b$  is varied so that condition  $\sum F_y = 0$  is met. On the schematics this process is not presented in detail, but is included in the purple boxes. The bubble velocity corrected forces are then used for a liftoff condition, that is when

$$\sum F_x = F_{st,x} + F_{gr,x} + F_{lift} + F_{bouy} > 0. \quad (10)$$

## 3 RESULTS

Given the methodologies described and the constants implemented, we now present the observed behaviors of the model.

### 3.1 Model analysis

To test the models behavior individual forces in stream-wise and wall-normal direction are presented in Figure 3. On x-axis the bubble diameter is shown in logarithmic scale. On y-axis the absolute value of forces is shown in logarithmic scale. Blue forces are acting in counter stream-wise direction or towards the wall, therefore, are keeping the bubble from departing. Red forces are acting in stream-wise or wall-normal direction, and are pushing the bubble to either slide or lift-off from the wall. The sum of forces is presented in black color.

On the left side we can observe the forces in stream-wise direction. The dominant force for small bubbles is  $F_{gr}$ . When bubble size increases,  $F_{gr}$  decreases, and  $F_{drag}$  increases significantly, being close to  $F_{gr}$ , as the  $\sum F_x \rightarrow 0$ . At this point the conditions for departure by sliding are satisfied, and the diameter where this happens is called sliding diameter ( $d_{ds}$ ). If the bubble size still increases, the  $F_{drag}$  begins to fall, following the  $F_{gr}$  closely. This is because the bubble sliding velocity is limiting the drag force, keeping the  $\sum F_x \rightarrow 0$ .

On the right side we can observe the forces in wall-normal direction. The dominant force for small bubbles is again  $F_{gr}$ . At some point around 2 mm all forces become relevant. Around that point, the sum of forces  $\sum F_x \rightarrow 0$ , and the conditions for bubble departure by liftoff are met. This diameter is called lift-off diameter ( $d_{dl}$ ). If the diameter further increases, the sum of forces increases again, this is because of absolute the values required for a log-log scale, the sum of forces has changed sign, and is pushing the bubbles away from the heated surface.

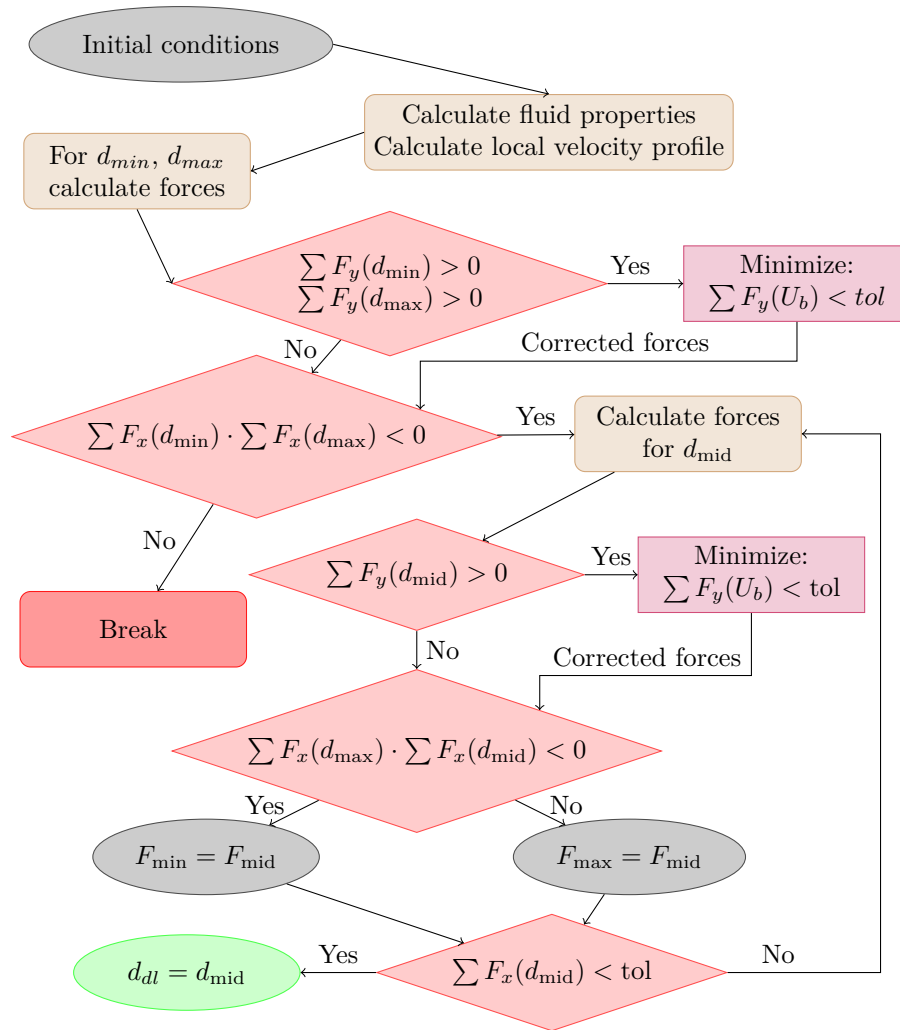


Figure 2: Schematics of the bisection minimization process to calculate the bubble lift off diameter for a given initial conditions and prescribed limits  $d_{min}$  and  $d_{max}$ . The oval shape represents the update of conditions, rectangles represent calculation processes, rhombus the decision, green oval the success and red rectangle the failing of the process. The purple rectangle represents another bisection algorithm used to calculate the bubble sliding velocity.

For the purpose of finding the boiling parameters we are not interested of individual forces, but the values of  $d_{ds}$  and particularly  $d_{dl}$ . In Figure 4, we can observe the sensitivity of the model to key flow parameters  $T_{sup}$ ,  $U_l$ , and  $p$ . On each graph an analysis has been performed by varying one parameter and keeping the other two constant. The sum of the forces near the point of interest, that is  $d_{ds}$  in dashed lines and  $d_{dl}$  in solid lines is presented. We can observe that under this conditions, the departure by sliding always happens before the departure by liftoff. In Figure 4 a) we can observe that the increase of  $T_{sup}$  increases  $F_{gr}$ , pushing both  $d_{ds}$  and  $d_{dl}$  towards bigger sizes as expected. Increasing  $U_l$  as shown Figure 4 b) affects both  $F_{drag}$  and  $F_{lift}$  pushing bubble  $d_{ds}$  and  $d_{dl}$  towards bigger sizes. Increasing  $p$  affects all forces by drastically changing thermal-physical properties of especially vapour phase. In Figure 4 c) we can observe a significant difference of  $d_{ds}$  but much less than expected in  $d_{dl}$ . Suspected reason for that is inadequate modeling of the constant  $d_w$  and the  $F_{st}$ . Since  $F_{st,x}$  is around order of magnitude smaller than  $F_{st,y}$  (look Figure 3), the  $d_{ds}$  is less affected than  $d_{dl}$ . Further analysis will be required to understand this behavior.

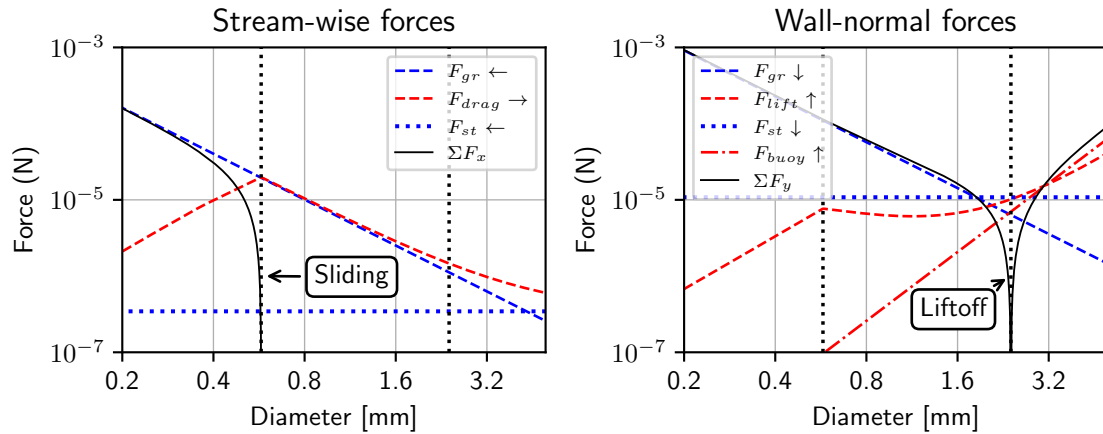


Figure 3: Log-log graph of forces acting on a growing bubble at the wall in water at  $p = 1$  bar and  $T_{sup} = 10$  K and  $U_l = 1$  m/s. The arrows and the color of the force indicate the direction of the force vector.

- Left) Forces acting in stream-wise direction. Black plot is a sum of forces, and its null indicates the sliding diameter.
- Right) Forces acting in wall-normal direction. Black plot is a sum of forces, and its null indicates the lift-off diameter.

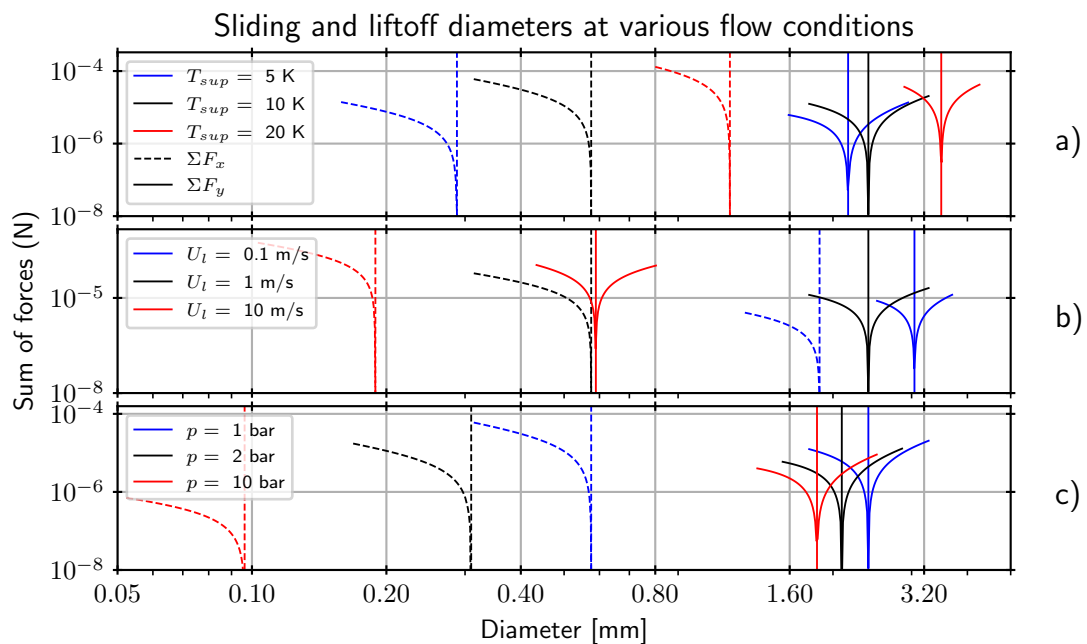


Figure 4: Sum of forces in stream-wise (dashed) and wall-normal (line) directions, in log-log scale. Minimums representing the departure by sliding diameter (dashed) and departure by lift-off diameter (line), respectively. The individual graphs represent:

- Sum of forces at  $p = 1$  bar and  $U_l = 1$  m/s, at three different wall super-heats.
- Sum of forces at  $p = 1$  bar and  $T_{sup} = 10$  K, at three different mean liquid velocities.
- Sum of forces at  $T_{sup} = 10$  K and  $U_l = 1$  m/s, at three different pressures.

### 3.2 Departure diameters

We can extend the calculations introduced in previous chapter, to the broader range of operating conditions. In this section the bubble liftoff departure diameters  $d_{dl}$  dependency on the key flow parameters will be presented over a broad range of operating conditions. To better understand the behavior of the model,  $d_{dl}$  is presented as a function of one parameter, while the second was varied between smaller, medium, and larger value, and third one was kept as a constant.

In Figure 5 a) we can observe the effect of increasing  $U_l$  at three different  $T_{sup}$ . Increasing the  $U_l$  decreases the  $d_{dl}$  and increasing  $T_{sup}$  increases it.

In Figure 5 b) we can observe the effect of increasing  $p$  at three different  $T_{sup}$ . Increasing the  $p$  decreases the  $d_{dl}$  until some point at around  $p = 4$  bar. After that, the departure diameter remained constant. Increasing  $T_{sup}$  had a significant increase in  $d_{dl}$  at low  $p$ , but none after some point.

In Figure 5 c) we can observe the effect of increasing  $T_{sup}$  at three different  $p$ . Increasing the  $T_{sup}$  results in a significant increase in the  $d_{dl}$ . Increasing the  $U_l$  pushes the bubble sizes towards smaller  $d_{dl}$ .

In Figure 5 d) we can observe the effect of increasing  $p$  at three different  $U_l$ . Increasing the pressure has some effect at low pressures, but none after some point. Increasing the velocity has a significant effect on  $d_{dl}$ .

In Figure 5 e) we can observe the effect of increasing  $T_{sup}$  at three different  $p$ . While the effects of  $T_{sup}$  is significant at low pressure (blue), it is less significant at medium (black) and negligible at high pressure (red).

In Figure 5 f) we can observe the effect of increasing  $U_l$  at three different  $p$ . The effects of  $U_l$  are significant, and very similar across all  $p$  ranges. Increase of  $p$  has a negligible effect on  $d_{dl}$ .

Based on the observed results, the model seems to be behaving reasonably at lower pressure ranges, but less reasonably at large pressures, where the effects of  $T_{sup}$  and  $U_l$  become negligible. This could be the result of inadequate modeling of surface tension force as discussed in a previous chapter.

### 3.3 CONCLUSIONS

A mechanistic model for calculation of bubble liftoff departure diameter was presented in this work. The model's behavior analysis has been performed, to gain a deeper understanding of the process behind the calculation of bubble sliding diameter and bubble liftoff diameter.

The model has been deployed to calculate the lift off diameter as a function of key flow parameters, that is: liquid velocity, pressure and wall super-heat. At low pressures the effects of wall super-heat and liquid velocity seem reasonable. A significant drawback seems to be the lesser sensitivity of the model at higher pressures. A potential reason for that is over prediction of surface tension force and the inadequate modeling of bubble contact diameter.

### ACKNOWLEDGMENTS

The financial support provided by the Slovenian Research Agency, grants P2-0026 and P2-0405 are gratefully acknowledged. This work was supported by the Helmholtz European Partnering Program in the project "Crossing borders and scales (Crossing)".

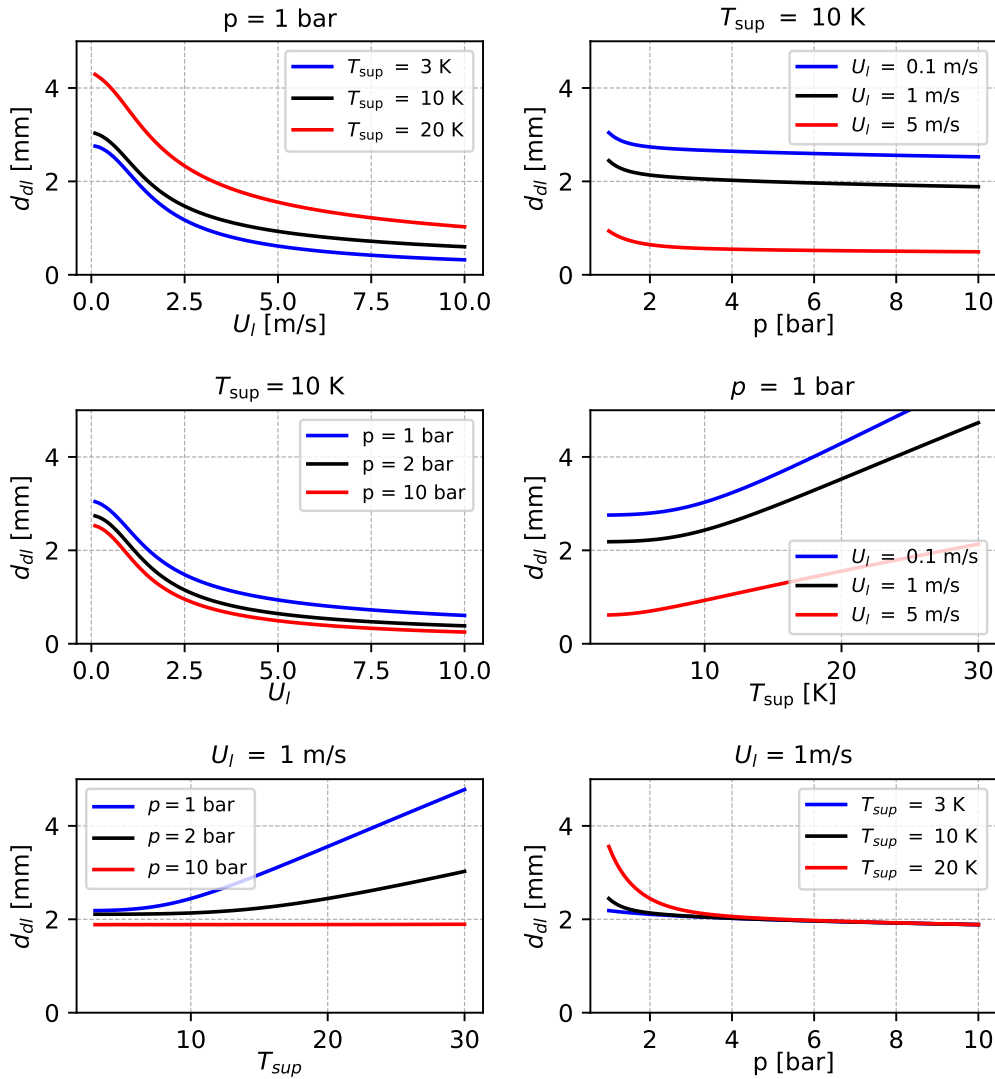


Figure 5: Dependency of  $d_{dl}$  on key flow parameters  $T_{sup}$ ,  $U_l$ , and  $p$ , across a large span of operating conditions. On each figure one is set as an x-variable, one is varied between smaller (blue) medium (black) and larger (red) value, and third was kept as a constant.

## REFERENCES

- [1] J.F. Klausner, R. Mei, D.M. Bernhard, and L.Z. Zeng. Vapor bubble departure in forced convection boiling. *International Journal of Heat and Mass Transfer*, 36(3):651–662, 1993.
- [2] L.Z. Zeng, J.F. Klausner, and R. Mei. A unified model for the prediction of bubble detachment diameters in boiling systems—i. pool boiling. *International Journal of Heat and Mass Transfer*, 36(9):2261–2270, 1993.
- [3] L.Z. Zeng, J.F. Klausner, D.M. Bernhard, and R. Mei. A unified model for the prediction of bubble detachment diameters in boiling systems—ii. flow boiling. *International Journal of Heat and Mass Transfer*, 36(9):2271–2279, 1993.
- [4] M.A. Rafiq Akand, Kei Kitahara, Tatsuya Matsumoto, Wei Liu, and Koji Morita. Experimental study and modeling of bubble lift-off diameter in subcooled flow boiling including the inclination effect of the heating surface. *Journal of Nuclear Science and Technology*, 58(11):1195–1209, 2021.

- [5] D. Mitrakos, A. Vouros, H. Bougioukou, and G. Giustini. Computational fluid dynamics prediction of subcooled boiling of water using a mechanistic bubble-departure model. *Nuclear Engineering and Design*, 412:112465, 2023.
- [6] Jingyu Du, Chenru Zhao, and Hanliang Bo. Investigation of bubble departure diameter in horizontal and vertical subcooled flow boiling. *International Journal of Heat and Mass Transfer*, 127:796–805, 2018.
- [7] M.G. Cooper and A.J.P. Lloyd. The microlayer in nucleate pool boiling. *International Journal of Heat and Mass Transfer*, 12(8):895–913, 1969.
- [8] Roland Clift, J Grace, and M Weber. *Bubbles, Drops, and Particles*. 01 1978.
- [9] T. R. Auton. The lift force on a spherical body in a rotational flow. *Journal of Fluid Mechanics*, 183:199–218, 1987.
- [10] Rong Situ, Takashi Hibiki, Mamoru Ishii, and Michitsugu Mori. Bubble lift-off size in forced convective subcooled boiling flow. *International Journal of Heat and Mass Transfer*, 48(25):5536–5548, 2005.
- [11] Ian H. Bell, Jorrit Wronski, Sylvain Quoilin, and Vincent Lemort. Pure and pseudo-pure fluid thermophysical property evaluation and the open-source thermophysical property library coolprop. *Industrial & Engineering Chemistry Research*, 53(6):2498–2508, 2014.